

Resonant enhancement of thermoelectric properties by correlated hopping for the Falicov-Kimball model on Bethe lattice

D. A. Dobushovskiy, A. M. Shvaika

Institute for Condensed Matter Physics of the National Academy of Sciences of Ukraine, Lviv, 79011 Ukraine

V. Zlatić

Institute of Physics, Zagreb POB 304, Croatia and

Department of Physics, Georgetown University, Washington, DC 20057, USA

The effect of correlated hopping on the charge and heat transport of strongly correlated particles is studied for the Falicov-Kimball model on the Bethe lattice. An exact solutions for the one particle density of states (DOS) and the two particle transport function (the “quasiparticle” scattering time) are derived using the dynamical mean field theory. For a wide range of the correlated hopping parameter, we find that the transport function that enters the Boltzmann relations for transport coefficients exhibits singularities due to the two particle resonant contributions, whereas the one particle DOS does not show any anomalous features. By tuning the number of itinerant electrons and bringing the Fermi level in the vicinity of the resonant frequency, we get a large increase of the conductivities and the thermoelectric power. Besides, when the hopping amplitude between the occupied sites is strongly reduced, the itinerant electrons localize in the clusters of sites occupied by f -electrons, which gives rise to an additional narrow band in the DOS, between the lower and upper Hubbard bands. This localized band has only a minor effect on the thermoelectric properties.

PACS numbers: 72.15.Jf, 72.20.Pa, 71.27.+a, 71.10.Fd

I. INTRODUCTION

The effects of electron correlations on various phenomena in different materials, from the one- and two-dimensional organic conductors, through three-dimensional solids, up to the optical lattices, are attracting a considerable interest for more than half a century. The majority of publication considered only the local Coulomb correlations of the Hubbard or Anderson type, $U \sum_i \hat{n}_{i\uparrow} \hat{n}_{i\downarrow}$. However, as noticed by Hubbard in his seminal article,¹ the second quantized representation of the inter-electron Coulomb interaction should also take into account, besides the local term, the nonlocal contributions. He pointed to the inter-site Coulomb interaction $\sum_{ij} V_{ij} \hat{n}_i \hat{n}_j$ and the so-called correlated hopping

$$\sum_{ij\sigma} t_{ij}^{(2)} (\hat{n}_{i\bar{\sigma}} + \hat{n}_{j\bar{\sigma}}) c_{i\sigma}^\dagger c_{j\sigma} \quad \text{and} \quad \sum_{ij\sigma} t_{ij}^{(3)} \hat{n}_{i\bar{\sigma}} c_{i\sigma}^\dagger c_{j\sigma} \hat{n}_{j\bar{\sigma}}, \quad (1)$$

which reflects the fact that the overlap of different many-body states is not the same, so that the value of inter-site hopping depends on the occupation of these states. The origin of the correlated hopping can either be a direct inter-site interaction or an indirect effective one.^{2,3} The problems arising from the local Coulomb interaction are the subject of famous Hubbard model which is widely investigated in the theory of strongly correlated electron systems.

The correlated hopping attracted much less attention.⁴ It was considered in connection with the new mechanisms of high temperature superconductivity,^{5,6} properties of organic compounds⁷ and molecular crystals,⁸ electron-hole asymmetry,⁹ and enhancement of magnetic properties.¹⁰ Recently, the correlated hopping has

been examined in relation to the quantum dots^{11–13} and fermionic^{14,15} and bosonic^{16–18} atoms on optical lattices.

Due to its nonlocal character, the correlated hopping is difficult to treat theoretically and the exact results, derived for some special cases, are of great importance, as they can be used for benchmarking various approximations. The simplest model of strongly correlated electrons is the Falicov-Kimball model¹⁹ which considers the local interaction between the itinerant d electrons and localized f electrons. It is a binary alloy type model and its ground state phase diagram for the one-dimensional ($D = 1$) and two-dimensional ($D = 2$) cases displays a variety of modulated phases.^{20–23} On the other hand, the dynamical mean field theory (DMFT)^{24–26} yields an exact solution of the Falicov-Kimball model in infinite dimensions, based on which the phase diagram and phase transitions in ordered phase were investigated and different spectral functions and responses were calculated.²⁷ The extension to correlated hopping was also considered and the DMFT solutions with a nonlocal self-energy were obtained.^{28–30}

In this article we study the effect of correlated hopping on the charge and heat transport for the Falicov-Kimball model on the Bethe lattice. The correlated hopping makes the Falicov-Kimball model similar to the binary alloy model with off-diagonal disorder³¹ which was studied long ago by Hoshino and Niizeki.³² Using the Mott’s relation and considering the special case of the hopping matrix with zero determinant (see below) they obtained the thermoelectric power of the model. More recently,³³ the general case of the hopping matrix was addressed on a $D \rightarrow \infty$ hypercubic lattice with the Gaussian density of states (DOS). Unfortunately, the Gaussian DOS possesses several difficulties related to the infinite bandwidth

(the interacting DOS decreases exponentially) and finite “quasiparticle” scattering time at $\omega \rightarrow \pm\infty$.³⁴ On the other hand, the Bethe lattice with semi-elliptic density of states has a finite bandwidth and zero “quasiparticle” scattering time whenever the DOS is zero, so it is much closer to the real three-dimensional systems.³⁵ In this paper, we calculate the single particle and the two particle properties and show that, unlike the single particle density of states, the transport properties show a number of surprising features due to the correlated hopping. In the $D = \infty$ Falicov-Kimball model, the phase transitions to the ordered phases could occur at very low temperatures but since the phase diagram for the model with correlated hopping is not known, we present the results obtained for the homogeneous phase all the way down to $T = 0$.

The paper is organized as follows. In section II, we present the DMFT solutions for the Falicov-Kimball model with correlated hopping on Bethe lattice. Section III provides derivation of the charge and energy transport coefficients in the homogeneous phase. In section IV we consider peculiarities of the charge and heat transport when we change the value of correlated hopping and doping. The results are summarized in section V.

II. DMFT FORMALISM FOR CORRELATED HOPPING ON BETHE LATTICE

A. The model Hamiltonian

The Hamiltonian of the Falicov-Kimball model¹⁹ with correlated hopping has the form

$$\begin{aligned} H &= H_{\text{loc}} + H_t, \\ H_{\text{loc}} &= \sum_i [U n_{id} n_{if} - \mu_f n_{if} - \mu_d n_{id}], \\ H_t &= \sum_{\langle ij \rangle} \frac{t_{ij}^*}{\sqrt{Z}} \left[t_1 d_i^\dagger d_j + t_2 d_i^\dagger d_j (n_{if} + n_{jf}) \right. \\ &\quad \left. + t_3 d_i^\dagger d_j n_{if} n_{jf} \right], \end{aligned} \quad (2)$$

where H_{loc} describes local correlations between the itinerant d -electrons and localized f -electrons and H_t collects nonlocal terms on the Bethe lattice with infinite coordination number $Z \rightarrow \infty$ including the nearest-neighbor inter-site hopping with amplitude t_1 and non-local correlations with amplitudes t_2 and t_3 — the so-called correlated hopping. Because the number of localized states is conserved, $[n_{if}, H] = 0$, one can introduce the projection operators $P_i^+ = n_{if}$ and $P_i^- = 1 - n_{if}$, and define the projected d -electron operators

$$\mathbf{d}_i = \begin{pmatrix} P_i^+ d_i \\ P_i^- d_i \end{pmatrix}, \quad (3)$$

such that the nonlocal term assumes the matrix form,²⁹

$$\begin{aligned} H_t &= \sum_{\langle ij \rangle} \frac{t_{ij}^*}{\sqrt{Z}} \left[t^{++} P_i^+ d_i^\dagger d_j P_j^+ + t^{--} P_i^- d_i^\dagger d_j P_j^- \right. \\ &\quad \left. + t^{+-} P_i^+ d_i^\dagger d_j P_j^- + t^{-+} P_i^- d_i^\dagger d_j P_j^+ \right] \\ &= \sum_{\langle ij \rangle} \frac{t_{ij}^*}{\sqrt{Z}} \mathbf{d}_i^\dagger \mathbf{t} \mathbf{d}_j, \end{aligned} \quad (4)$$

where the hopping matrix is

$$\mathbf{t} = \begin{pmatrix} t^{++} & t^{+-} \\ t^{-+} & t^{--} \end{pmatrix} \quad (5)$$

and the connection between the hopping matrix elements and the initial hopping amplitudes reads

$$\begin{aligned} t^{--} &= t_1, & t_1 &= t^{--}, \\ t^{+-} &= t^{-+} = t_1 + t_2, & t_2 &= t^{+-(-+)} - t^{--}, \\ t^{++} &= t_1 + 2t_2 + t_3, & t_3 &= t^{++} + t^{--} - t^{+-} - t^{-+}. \end{aligned} \quad (6)$$

Our aim is to find the transport properties of the model. As shown below, in the limit of large coordination number, the transport coefficients are related to single particle Green’s function.

B. The single particle Green’s function

The off-diagonal Green’s function for projected d -electrons is defined by the matrix $\mathbf{G}_{ij} = \|\mathbf{G}_{ij}^{\alpha\beta}\|$, where $\alpha, \beta = \pm$. On the imaginary time-axis we have

$$\mathbf{G}_{ij}(\tau - \tau') = - \left\langle \mathcal{T} \mathbf{d}_i(\tau) \otimes \mathbf{d}_j^\dagger(\tau') \right\rangle, \quad (7)$$

where \mathcal{T} is the imaginary-time ordering operator, \otimes denotes the direct (Cartesian) product of two vectors and the angular bracket denotes the quantum statistical averaging with respect to H . The Green’s function is calculated by treating H_t as perturbation, i.e., by expanding around the atomic limit. This leads to the Dyson-type equation which can be written in the matrix form as

$$\mathbf{G}_{ij}(\omega) = \Xi_{ij}(\omega) + \sum_{\langle i'j' \rangle} \Xi_{ij'}(\omega) \cdot \frac{t_{j'i'}^*}{\sqrt{Z}} \mathbf{t} \cdot \mathbf{G}_{i'j}(\omega), \quad (8)$$

where $\Xi_{ij}(\omega)$ is the irreducible cumulant^{26,36} which cannot be split into two disconnected parts by removing a single hopping line. In the $Z \rightarrow \infty$ limit, the irreducible part becomes local

$$\Xi_{ij}(\omega) = \delta_{ij} \Xi(\omega) \quad (9)$$

and can be computed by the DMFT. In that approach, the local Green’s functions of the lattice is equated with the Green’s functions of an auxiliary impurity embedded in the self-consistent environment described by the

time-dependent mean fields (λ -fields). Introducing the unperturbed DOS of the Bethe lattice in the $Z = \infty$ limit,

$$\rho(\epsilon) = \frac{2}{\pi W^2} \sqrt{W^2 - \epsilon^2}, \quad (10)$$

we can write the DMFT equation in the matrix form as²⁹

$$\begin{aligned} \mathbf{G}_{\text{local}}(\omega) &\equiv \mathbf{G}_{ii}(\omega) = \int_{-\infty}^{+\infty} d\epsilon \rho(\epsilon) \mathbf{G}_{\epsilon}(\omega) \\ &= [\mathbf{\Xi}^{-1}(\omega) - \mathbf{\Lambda}(\omega)]^{-1} = \mathbf{G}_{\text{imp}}(\omega), \end{aligned} \quad (11)$$

where $\mathbf{\Lambda}(\omega) = \|\lambda^{\alpha\beta}(\omega)\|$ is the matrix of λ -fields, $\mathbf{G}_{\text{imp}}(\omega)$ is Green's function for the auxiliary impurity problem, and

$$\mathbf{G}_{\epsilon}(\omega) = [\mathbf{\Xi}^{-1}(\omega) - \mathbf{t}\epsilon]^{-1}, \quad (12)$$

is the lattice Green's function matrix. It is defined by its components

$$G_{\epsilon}^{\beta\alpha}(\omega) = \frac{A_{\beta\alpha}(\omega) - B_{\beta\alpha}\epsilon}{C(\omega) - D(\omega)\epsilon + \epsilon^2 \det \mathbf{t}}, \quad (13)$$

where we introduced the matrix adjugate to $\mathbf{\Xi}^{-1}(\omega)$,

$$\mathbf{A}(\omega) = \text{adj } \mathbf{\Xi}^{-1}(\omega) = \mathbf{\Xi}(\omega) / \det \mathbf{\Xi}(\omega) \quad (14)$$

and the matrix adjugate of the hopping matrix \mathbf{t} ,

$$\mathbf{B} = \text{adj } \mathbf{t} = \mathbf{t}^{-1} \det \mathbf{t}, \quad (15)$$

while the scalars C and D are given by

$$C(\omega) = \det \mathbf{A}(\omega) = \det \mathbf{\Xi}^{-1}(\omega) = 1 / \det \mathbf{\Xi}(\omega), \quad (16)$$

and

$$D(\omega) = \text{Tr} [\mathbf{A}(\omega) \mathbf{t}] = \text{Tr} [\mathbf{\Xi}^{-1}(\omega) \mathbf{B}]. \quad (17)$$

The DMFT equation (11) contains two unknowns: the irreducible part $\mathbf{\Xi}(\omega)$ and the dynamical mean field $\mathbf{\Lambda}(\omega)$, both of which follow from $\mathbf{G}_{\text{imp}}(\omega)$. For the Falicov-Kimball model with correlated hopping, we have

$$\begin{aligned} G_{\text{imp}}^{++}(\omega) &= w_1 g_1(\omega), \\ G_{\text{imp}}^{--}(\omega) &= w_0 g_0(\omega), \\ G_{\text{imp}}^{+-}(\omega) &= G_{\text{imp}}^{-+}(\omega) = 0, \end{aligned} \quad (18)$$

where $w_1 = \langle P^+ \rangle = \langle n_f \rangle$, $w_0 = \langle P^- \rangle = \langle 1 - n_f \rangle$, and

$$\begin{aligned} g_0(\omega) &= \frac{1}{\omega + \mu_d - \lambda^{--}(\omega)}, \\ g_1(\omega) &= \frac{1}{\omega + \mu_d - U - \lambda^{++}(\omega)} \end{aligned} \quad (19)$$

are the impurity Green's functions in the absence and the presence of f -particle, respectively. From $\mathbf{G}_{\text{imp}}(\omega)$, we also compute the renormalized density of states,

$$\begin{aligned} A_d(\omega) &= -\frac{1}{\pi} \sum_{\alpha, \beta = \pm} \text{Im } G_{\text{imp}}^{\alpha\beta}(\omega) \\ &= -\frac{1}{\pi} [w_0 \text{Im } g_0(\omega) + w_1 \text{Im } g_1(\omega)]. \end{aligned} \quad (20)$$

Note, for the Bethe lattice, the DMFT equation (11) simplifies to²⁹

$$\mathbf{\Lambda}(\omega) = \frac{W^2}{4} \mathbf{t} \mathbf{G}_{\text{imp}}(\omega) \mathbf{t}. \quad (21)$$

In what follows, we use $W = 2$, which defines our energy scale in numerical calculations. Substituting Eq. (19) in Eq. (21) yields a system of equations

$$\begin{aligned} \omega + \mu_d - U - \frac{1}{g_1(\omega)} &= \frac{W^2}{4} [(t^{++})^2 w_1 g_1(\omega) + (t^{+-})^2 w_0 g_0(\omega)], \\ \omega + \mu_d - \frac{1}{g_0(\omega)} &= \frac{W^2}{4} [(t^{+-})^2 w_1 g_1(\omega) + (t^{--})^2 w_0 g_0(\omega)] \end{aligned} \quad (22)$$

which, in general, provide the 4th order polynomial equations for $g_0(\omega)$ and $g_1(\omega)$.

Previous investigations of the Falicov-Kimball model with correlated hopping²⁹ have shown that the shape of the renormalized DOS and the transport properties depend strongly on the structure of hopping matrix (5), and that one can distinguish five different cases (in what follows, unless stated explicitly, we take $t^{--} = t_1 = 1$):

- (a) For $t^{++} \neq 0$, $t^{+-} \neq 0$, and $\det \mathbf{t} = 0$, the right-hand parts of equations (22) are proportional to each other, so that

$$\begin{aligned} \frac{1}{t^{++}} \left[\omega + \mu_d - U - \frac{1}{g_1(\omega)} \right] &= \frac{1}{t^{--}} \left[\omega + \mu_d - \frac{1}{g_0(\omega)} \right] \\ &= \frac{W^2}{4} [t^{++} w_1 g_1(\omega) + t^{--} w_0 g_0(\omega)]; \end{aligned} \quad (23)$$

Note, the regular Falicov-Kimball model without the correlated hopping belongs also to this case;

- (b) For $t^{++} = 0$, $t^{+-} \neq 0$, and $\det \mathbf{t} \neq 0$, one of the diagonal components of the hopping matrix vanish, so that the direct hopping of d -particles between the sites occupied by the f -particles is reduced;
- (c) For $t^{++} \neq 0$, $t^{+-} = 0$, and $\det \mathbf{t} \neq 0$, the hopping matrix is diagonal and the hopping of d -particles is allowed only between the sites with the same occupation of f -states;

- (d) For $t^{++} = 0$, $t^{+-} = 0$, and $\det \mathbf{t} = 0$ we are dealing with the simultaneous realization of all three previous cases, and the hopping of d -particles is allowed only between the sites which are *not* occupied by the f -particles;
- (e) The most general case is obtained for $t^{++} \neq 0$, $t^{+-} \neq 0$, $\det \mathbf{t} \neq 0$.

For the cases (a,b) and (c,d), the impurity Green's functions $g_0(\omega)$ and $g_1(\omega)$ are defined by cubic and a quadratic equations, respectively. Within the solutions of these equations we choose only the one which corresponds to the retarded Green's functions with negative imaginary parts. For the general case (e), the quartic polynomial equation with real coefficients has either four real roots, or two real and two mutually conjugated complex roots. The correct physical solution is the one which gives both retarded Green's functions $g_0(\omega)$ and $g_1(\omega)$ with negative imaginary parts. It can be shown that there is only one set of physical solutions. When ω has only the real roots, the physical solution is obtained by using the spectral relation

$$\text{Re } g_{0,1}(\omega) = -\frac{1}{\pi} \int_{-\infty}^{+\infty} d\omega' \frac{\text{Im } g_{0,1}(\omega')}{\omega - \omega'}, \quad (24)$$

which yields the correct retarded Green's functions and the renormalized single-particle density of states.

For the local single-particle Green's function

$$G_{ii}(\tau - \tau') = -\left\langle \mathcal{T} d_i(\tau) d_i^\dagger(\tau') \right\rangle, \quad (25)$$

we have

$$\begin{aligned} G_{ii}(\omega) &= \sum_{\alpha, \beta = \pm} G_{\text{imp}}^{\alpha\beta}(\omega) = w_0 g_0(\omega) + w_1 g_1(\omega) \\ &= [\omega - \Sigma(\omega) - \lambda_{\text{HF}}(\omega)]^{-1}, \end{aligned} \quad (26)$$

where $\lambda_{\text{HF}}(\omega) = w_1 \lambda^{++}(\omega) + w_0 \lambda^{--}(\omega)$ is the Hartree-Fock dynamical mean field, and

$$\Sigma(\omega) = U w_1 + \frac{\tilde{U}^2(\omega) w_1 w_0}{\omega - \tilde{U}(\omega) w_0 - \lambda^{--}(\omega)} \quad (27)$$

is local self-energy, which is different from the nonlocal one for the lattice Green's function.²⁹ The parameter

$$\tilde{U}(\omega) = U + \lambda^{++}(\omega) - \lambda^{--}(\omega) \quad (28)$$

is an effective retarded Coulomb interaction. These expressions reveal the dual nature of correlated hopping: on one hand, it modifies the hopping amplitude in the Hartree-Fock term $\lambda_{\text{HF}}(\omega)$, and, on the other hand, it leads to the nonlocal two-particle correlation which gives rise to the retarded local interaction.

III. TRANSPORT COEFFICIENTS IN THE PRESENCE OF CORRELATED HOPPING

We now calculate the transport properties of correlated electrons using the linear response theory. The Falicov-Kimball model with correlated hopping satisfies the Boltzmann (Jonson-Mahan) theorem,^{33,37-39} so that all the transport coefficients can be obtained from the transport integrals defined by a single transport function,

$$\mathbf{L}_{lm} = \frac{\sigma_0}{e^2} \int_{-\infty}^{+\infty} d\omega \left[-\frac{df(\omega)}{d\omega} \right] \mathbf{I}(\omega) \omega^{l+m-2}, \quad (29)$$

where $f(\omega) = 1/(e^{\omega/T} + 1)$ is the Fermi distribution function and $\mathbf{I}(\omega)$ is the transport function which is given below.

The conductivity, the Seebeck coefficient (thermoelectric power $\mathbf{E} = \mathbf{S} \nabla T$), and the electronic contribution in thermal conductivity follow immediately from transport integrals as

$$\sigma_{\text{dc}} = e^2 \mathbf{L}_{11}, \quad (30)$$

$$\mathbf{S} = \frac{1}{eT} \mathbf{L}_{11}^{-1} \mathbf{L}_{12}, \quad (31)$$

$$\kappa_e = \frac{1}{T} [\mathbf{L}_{22} - \mathbf{L}_{21} \mathbf{L}_{11}^{-1} \mathbf{L}_{12}], \quad (32)$$

respectively.

The DMFT expression for the transport function generalized to the case of correlated hopping reads

$$\begin{aligned} I(\omega) &= \frac{1}{\pi} \int d\epsilon \rho(\epsilon) \Phi_{xx}(\epsilon) \text{Tr} [\mathbf{t} \text{Im } \mathbf{G}_\epsilon(\omega) \mathbf{t} \text{Im } \mathbf{G}_\epsilon(\omega)] \\ &= \frac{1}{\pi} \sum_{\alpha\beta\alpha'\beta'} t^{\alpha\beta} t^{\alpha'\beta'} \int d\epsilon \rho(\epsilon) \Phi_{xx}(\epsilon) \text{Im } G_\epsilon^{\beta\alpha'}(\omega) \text{Im } G_\epsilon^{\beta'\alpha}(\omega), \end{aligned} \quad (33)$$

where $\Phi_{xx}(\epsilon)$ is the so-called lattice-specific transport DOS.⁴⁰ For the $D = \infty$ hypercubic lattice with Gaussian DOS, we have $\Phi_{xx}(\epsilon) = W^2/2D$, whereas for the $Z = \infty$ Bethe lattice with the semielliptic DOS, the f -sum rule yields⁴¹

$$\Phi_{xx}(\epsilon) = \frac{1}{3Z} (W^2 - \epsilon^2). \quad (34)$$

The integral over ϵ in Eq. (33) can now be evaluated and the final result for the transport function depends on the value of $\det \mathbf{t}$.

For $\det \mathbf{t} = 0$, we find

$$I(\omega) = \frac{1}{2\pi} \left\{ \text{Re } \Psi' \left[\frac{C(\omega)}{D(\omega)} \right] - \frac{\text{Im } \Psi \left[\frac{C(\omega)}{D(\omega)} \right]}{\text{Im} \left[\frac{C(\omega)}{D(\omega)} \right]} \right\}, \quad (35)$$

where

$$\begin{aligned}\Psi(\zeta) &= \int d\epsilon \frac{\rho(\epsilon)}{\zeta - \epsilon} \Phi_{xx}(\epsilon), \\ \Psi'(\zeta) &= \frac{d\Psi(\zeta)}{d\zeta}.\end{aligned}\quad (36)$$

For the semielliptic DOS, we find

$$\begin{aligned}\Psi(\zeta) &= \frac{1}{3} [(W^2 - \zeta^2)F(\zeta) + \zeta], \\ \Psi'(\zeta) &= \frac{1}{3} [(W^2 - \zeta^2)F'(\zeta) + 1 - 2\zeta F(\zeta)],\end{aligned}\quad (37)$$

where

$$\begin{aligned}F(\zeta) &= \int d\epsilon \frac{\rho(\epsilon)}{\zeta - \epsilon} = \frac{2}{W^2} (\zeta - \sqrt{\zeta^2 - W^2}), \\ F'(\zeta) &= \frac{dF(\zeta)}{d\zeta} = \frac{\zeta F(\zeta) - 2}{\zeta^2 - W^2}.\end{aligned}\quad (38)$$

The transport function (35) is similar to the one for the Falicov-Kimball model without the correlated hopping, provided we replace the inverse irreducible part $\Xi^{-1}(\omega) = \omega + \mu_d - \Sigma(\omega)$ by the expression

$$\frac{C(\omega)}{D(\omega)} = \frac{1}{\text{Tr}[\Xi(\omega)\mathbf{t}]}.\quad (39)$$

For $\det \mathbf{t} \neq 0$, the transport function reads

$$\begin{aligned}I(\omega) &= \frac{1}{2\pi} \left[\text{Re} \{ \Psi'[E_1(\omega)] + \Psi'[E_2(\omega)] \} - \frac{\text{Im} \Psi[E_1(\omega)]}{\text{Im} E_1(\omega)} - \frac{\text{Im} \Psi[E_2(\omega)]}{\text{Im} E_2(\omega)} \right. \\ &\quad \left. - K(\omega) \left\{ \frac{1}{\text{Im} E_1(\omega)} \text{Im} \frac{\Psi[E_1(\omega)]}{[E_1(\omega) - E_2(\omega)][E_1(\omega) - E_2^*(\omega)]} + \frac{1}{\text{Im} E_2(\omega)} \text{Im} \frac{\Psi[E_2(\omega)]}{[E_2(\omega) - E_1(\omega)][E_2(\omega) - E_1^*(\omega)]} \right\} \right],\end{aligned}\quad (40)$$

where E_1 and E_2 are the roots of the denominator in Eq. (13), $C(\omega) - D(\omega)\epsilon + \epsilon^2 \det \mathbf{t} = 0$, given by

$$E_1(\omega) = \frac{D(\omega)}{2 \det \mathbf{t}} \left[1 + \sqrt{1 - \frac{4C(\omega)}{D^2(\omega)} \det \mathbf{t}} \right],\quad (41)$$

$$E_2(\omega) = \frac{2C(\omega)}{D(\omega)} \left[1 + \sqrt{1 - \frac{4C(\omega)}{D^2(\omega)} \det \mathbf{t}} \right]^{-1},\quad (42)$$

and $K(\omega)$ reads

$$K(\omega) = 2 \text{Re}[E_1(\omega)E_2^*(\omega)] - \frac{1}{\det \mathbf{t}} \text{Re} \text{Tr}[\mathbf{A}^*(\omega)\Xi^{-1}(\omega)].\quad (43)$$

In the limit $\det \mathbf{t} \rightarrow 0$, the eigenvalue E_1 diverges and its contribution in the transport function vanishes, whereas $E_2(\omega) \rightarrow C(\omega)/D(\omega)$, so that we recover the transport function given by expression (35).

IV. RESULTS

In the first part of this section we present the results for the dependence of the interacting density of states $A_d(\omega)$ and the transport function $I(\omega)$ on the frequency ω and correlated hopping t_2 . We show the data in the weak ($U = 0.25$) and the strong ($U = 2$) coupling regime, for different concentrations of f -particles. In the second part, we show the effect of correlated hopping on the transport coefficients in the weak and the strong coupling limit.

A. The density of states and the transport function

In the weak coupling limit ($U = 0.25$, $t_3 = 0$), the dependence of $A_d(\omega)$ and $I(\omega)$ on ω and t_2 is shown Fig. 1 in the false color plot. The concentration of the f particles varies from $n_f = 0.5$ to 0.9. The data show that band edges of $A_d(\omega)$ and $I(\omega)$ are the same and that the band width increases for $t_2 > 0$ and $t_2 < -1$, while it shrinks for $-1 < t_2 < 0$.

The DOS is a smooth and almost semi-elliptic function for all values of t_2 , except for $t_2 \approx -(t_1 + t_3)/2$ ($t_2 \approx -0.5$ for the case considered here, $t_3 = 0$), where the matrix element t^{++} becomes small and changes sign. At half-filling, $n_f = 0.5$, and in close vicinity of $t_2 = -0.5$ ($t^{++} = 0$), the DOS exhibits a tiny gap at $\omega = U$ [see the white dot in the insert in Fig. 1(b)], with sharp peak at the bottom-edge of the upper band [see Fig. 7 below]. For larger values of n_f , the DOS starts to develop more prominent gaps, creating, first, the two-band and, then, the three-band structure. In the case of the two-band structure, the spectral weights of the lower and upper bands are $w_0 = 1 - n_f$ and $w_1 = n_f$, respectively, which is similar to what one finds in the doped Mott-Hubbard insulator phase of the Falicov-Kimball model without correlated hopping.^{35,42,43} As we approach the $t^{++} = 0$ point, an additional gap appears in the upper Hubbard band and the two-peak structure is transformed into a three-peak one; the spectral weights of the lower and upper bands are the same $w_0 = 1 - n_f$, while the spectral weight of the middle band is $2n_f - 1$. For $t^{++} \rightarrow 0$, the

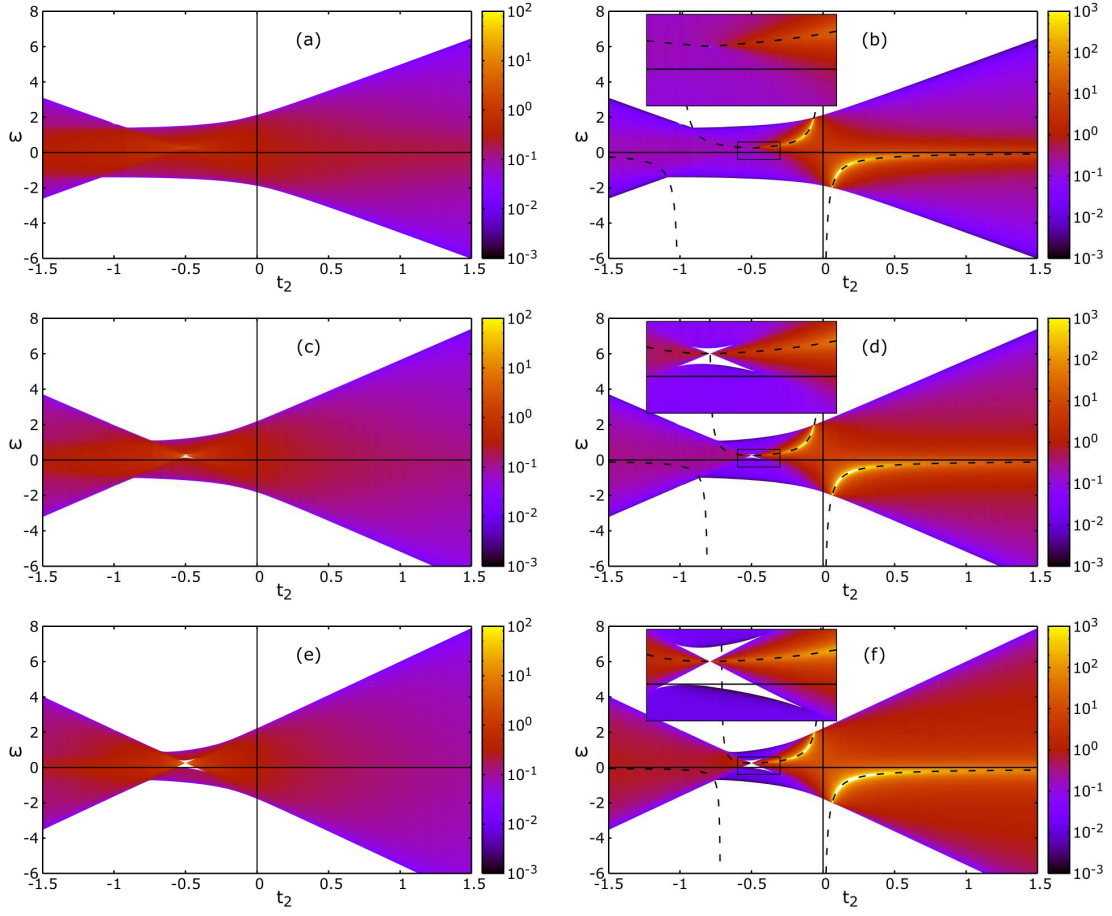


FIG. 1. (Color online) The density of states $A_d(\omega)$, left panels (a), (c), (e), and the transport function $I(\omega)$, right panels (b), (d), (f), shown as a function of frequency ω and correlated hopping parameter t_2 on a false color plot for $U = 0.25$, $t_3 = 0$, and for f -particle concentrations (a,b) $n_f = 0.5$, (c,d) 0.75 , and (e,f) 0.9 (top to bottom). Inserts represent enlarged rectangular areas in the vicinity of $t^{++} = 0$ and $\omega = U$. Dashed line indicates the resonant frequency ω_{res} given by Eq. (45).

DOS of the middle band narrows to a δ -peak.

The mid-band emerges because the probability of the neighboring sites being occupied by the f -particles becomes, for $n_f > 1/2$, macroscopically large, so that the clusters of sites occupied by the f -particles are created. At the same time, the values of t_2 are such that the hopping matrix element t^{++} is very small and direct hopping of d -particles is suppressed. Thus, the d -particles within the cluster are localized, producing a band of localized states which are separated from the upper Hubbard band by the localization gap. As $n_f \rightarrow 1$, almost all the sites are occupied by f -particles, so that the cluster covers the whole lattice and the weight of the lower and upper band decreases as $1 - n_f$, while the DOS is dominated by a narrow peak of localized states located at $\omega = U$. The presence of the clusters of localized states strongly affects the properties of itinerant d -electrons around the Fermi level (the chemical potential μ_d at zero temperature). For $n_d < 1 - n_f$, the Fermi level is in the lower band; for $1 - n_f < n_d < n_f$, it is fixed in the narrow mid-peak and the localized d -states of clusters are filled;

for $n_d > n_f$, the Fermi level is in the upper band.

In the strong coupling limit, the interacting DOS and the transport function are changed in a qualitative way. As shown in Fig. 2 (left panel), the Mott-Hubbard gap extends over larger values of t_2 , including the case without the correlated hopping (Mott transition in the regular Falicov-Kimball model). On the other hand, the localization band is pushed to the upper Hubbard band and becomes very narrow; the corresponding localization gap exists only in the close vicinity of the $t^{++} = 0$ value.

The transport function, shown in the right panel of Figs. 1 and 2, shows a completely different behavior than the density of states. For $t_2 > -(t_1 + t_3)/2$, and $t^{++} > 0$, the transport function exhibits a strong enhanced at $\omega = \omega_{\text{res}}$. Numerical analysis of Eq. (40) shows that the main contribution to $I(\omega)$ at $\omega \simeq \omega_{\text{res}}$ is coming from the term $\text{Im} \Psi[E_2(\omega)]/\text{Im} E_2(\omega)$. The resonant frequency ω_{res} corresponds to the λ -fields and the Green's functions such that

$$\frac{\lambda^{++}(\omega)}{\lambda^{--}(\omega)} = \frac{g_0(\omega)}{g_1(\omega)} = \eta, \quad (44)$$

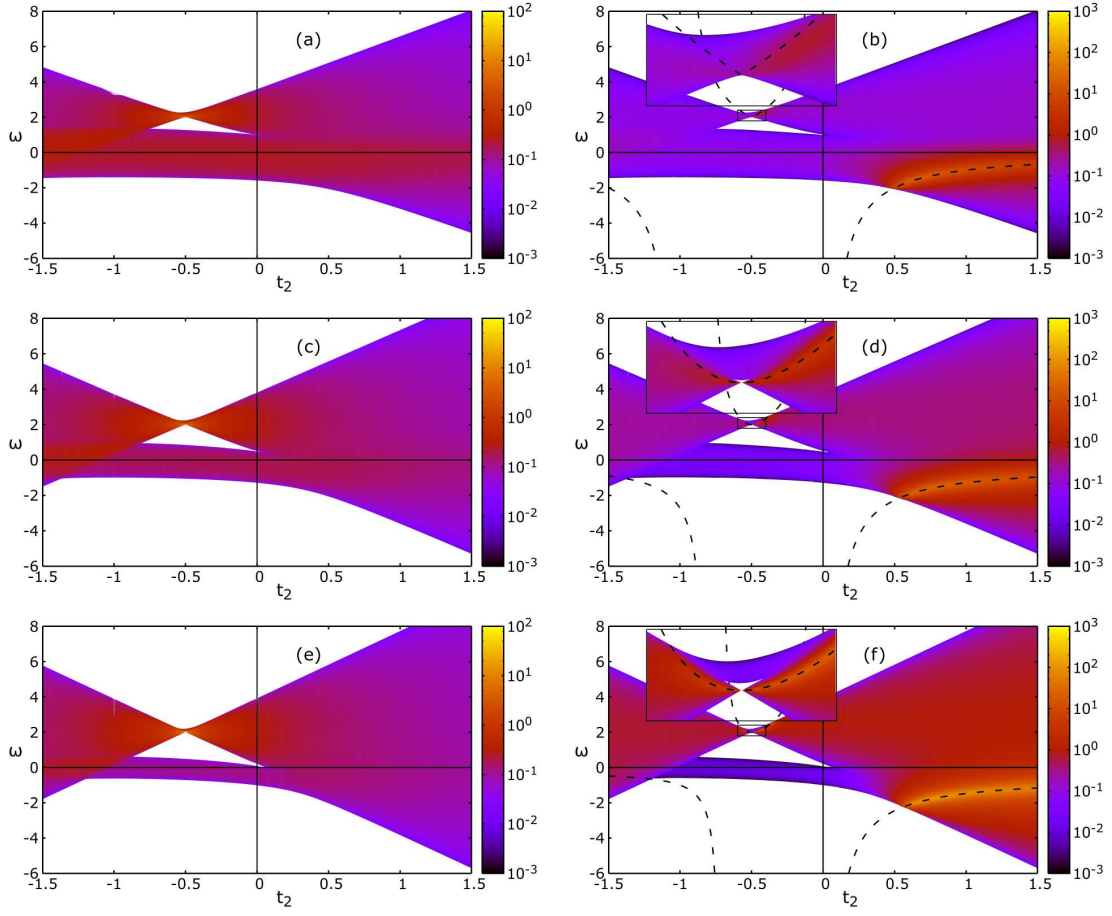


FIG. 2. (Color online) Same as in Fig. 1 for $U = 2$.

which gives

$$\omega_{\text{res}} = \frac{U}{1 - \eta} \quad (45)$$

with

$$\eta = \frac{(t^{+-})^2}{(t^{--})^2} - \frac{(t^{+-})^2 - \sqrt{(t^{+-})^4 + 4w_1w_0[(t^{++}t^{--})^2 - (t^{+-})^4]}}{2(t^{--})^2w_0}. \quad (46)$$

The resonant frequency is indicated in Figs. 1 and 2 by dashed lines. For two special values of t_2 , given by the solutions of the equation $\eta = 1$ or

$$(t^{--})^2w_0 + (t^{+-})^2(w_1 - w_0) - (t^{++})^2w_1 = 0, \quad (47)$$

the resonant frequency is shifted outside the bands and becomes infinite. The regular Falicov-Kimball model, where $t^{--} = t^{+-} = t^{++} = t_1$, is exactly at one of this special points with $\omega_{\text{res}} \rightarrow \pm\infty$, so that the transport function has no resonant contribution. On the other

hand, in the case $t^{++} \rightarrow 0$ and the d -electron localization, ω_{res} is within the localized band, so that the resonant contributions become prominent for $t^{++} > 0$ and are suppressed for $t^{++} < 0$.

Note, expressions (45) and (46) for the resonant frequency do not depend on parameter W characterizing the semi-elliptic DOS and continue to hold for other lattices with different unperturbed DOS, including the Gaussian one. However, the hypercubic lattice with the Gaussian DOS has no clear band edges and the resonant peak is within the band for any value of correlated hopping.³³ For $\eta = 1$, we have $\omega_{\text{res}} \rightarrow \infty$ and there are no resonant contributions to transport.

B. Transport coefficients

1. Weakly correlated hopping

In the weak coupling regime, the interaction constants are much smaller than the hopping integral: $|U|, |t_2|, |t_3| \ll |t_1|$. At half filling $n_f = n_d = 1/2$, the density of states $A_d(\omega)$ is a slightly deformed with respect to the unperturbed, semi-elliptic one, i.e., the cor-

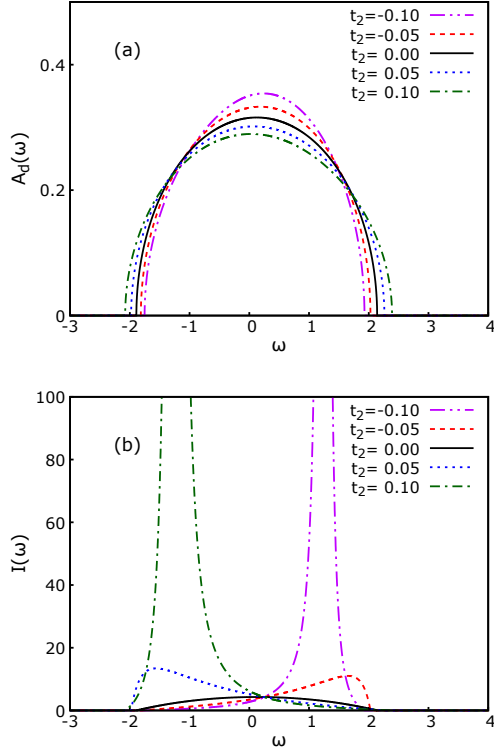


FIG. 3. (Color online) The interacting DOS (panel a) and the transport function (panel b) plotted versus frequency for $U = 0.25$ at half filling ($n_f = n_d = 1/2$) and for $t_2 = -0.1, -0.05, 0, 0.05, 0.1$ ($t_3 = 0$).

related hopping breaks the electron-hole symmetry and makes $A_d(\omega)$ asymmetric [see Fig. 3(a)]. The width of the conduction band increases for $t_2 > 0$ and decreases for $t_2 < 0$.

In contrast, the transport function $I(\omega)$, which is almost semi-elliptic in the absence of the correlated hopping, becomes highly asymmetric as soon as $t_2 \neq 0$. For $t_2 = \pm 0.05$, when the resonant peak is outside the conduction band, the transport function is somewhat enhanced close to the band edges but it is still a smooth and almost a flat function around the chemical potential, $\mu \sim U/2$ [see Fig. 3(b)]. Hence, the transport coefficients exhibit typical metallic behavior as functions of temperature (see Fig. 4). For $t_2 = \pm 0.1$, the resonant peak gives the main contribution to the transport function. At low temperatures, the resonant peak is outside the Fermi window, $-df(\omega)/d\omega|_{\omega \simeq \omega_{\text{res}}} \simeq 0$, and its contribution to the integral in Eq. (29) is negligibly small. Thus, the transport coefficients still exhibit the metallic behavior. However, as temperature increases and the resonant peaks enter the Fermi window, we observe, first, an enhancement of the thermal conductivity, then, of the thermoelectric power, and, eventually, of the electric conductivity (see Fig. 4).

In the weak coupling regime, the doping does not change much the shape of the DOS and the transport

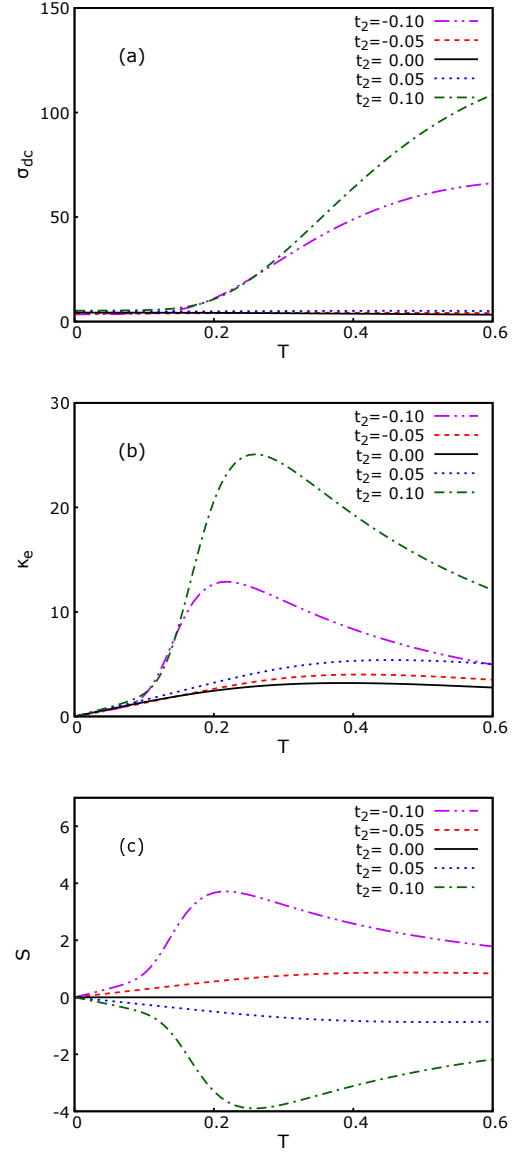


FIG. 4. (Color online) Temperature dependences of the dc conductivity σ_{dc} , thermal conductivity κ_e , and the Seebeck coefficient S for the same parameters as in Fig. 3.

function (see Fig. 5 for the case of $n_f = 0.75$ and $n_d = 0.25$). The main effect of the doping is the shift of the chemical potential to the bottom of conduction band, such that $\mu \sim -1$. For $t_2 = 0.1$, the resonant peak is in the vicinity of Fermi level and we find that the electric and thermal conductivity, and the thermopower are enhanced with respect to the half-filled case and with respect to the values of t_2 for which the resonant peak is absent (see Fig. 6). For $t_2 = -0.1$, the resonant peak is too far away from the chemical potential to contribute to the electric and thermal conductivity but the large asymmetry of $I(\omega)$, shown in Fig. 5(b), gives rise to a large thermopower at high temperatures.

As shown in Fig. 2, an increase of local Coulomb in-

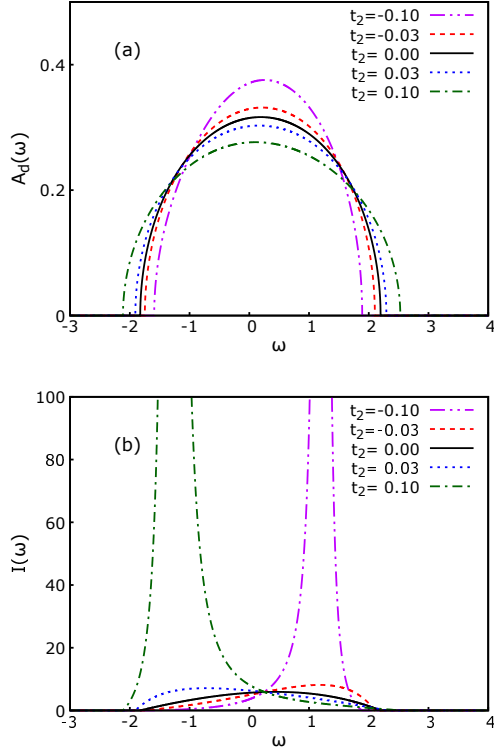


FIG. 5. (Color online) The interacting DOS (panel a) and the transport function (panel b) plotted versus frequency for $U = 0.25$, $n_f = 0.75$, and $n_d = 1 - n_f = 0.25$ and for $t_2 = -0.1, -0.03, 0, 0.03, 0.1$.

interaction U shifts the resonant frequency in the region of large positive and negative values of t_2 , so that the resonant peaks do not affect much the transport properties for small values of correlated hopping t_2 . The only effect of correlated hopping is to break the electron-hole symmetry and to make $A_d(\omega)$ and $I(\omega)$ asymmetric functions of ω . Hence, in this part of the parameter space, the transport coefficients behave similarly as in the case of the doped Falicov-Kimball model without correlated hopping.^{35,42,43}

A different behavior emerges for small values of the diagonal component t^{++} , when the direct hopping amplitude between the sites occupied by f -particles is much reduced, while the hopping between occupied and unoccupied, and between the unoccupied sites is large. For the Gaussian density of states, this case was analyzed in Ref. [33] (see Figs. 6 and 7 of Ref. [33]). For the semi-elliptic density of states, we find similar behavior but the data reveal more details and we discover new interesting regimes.

At half filling and $t^{++} = 0$ ($t_2 = -0.5$), the DOS acquires a tiny gap at the Fermi level, bounded by the singularity at the bottom of the upper Hubbard band [see Fig. 7(a)]. The transport function also displays a gap but the band-edge singularity is replaced by a step like function [Fig. 7(b)]. The presence of the gap at Fermi

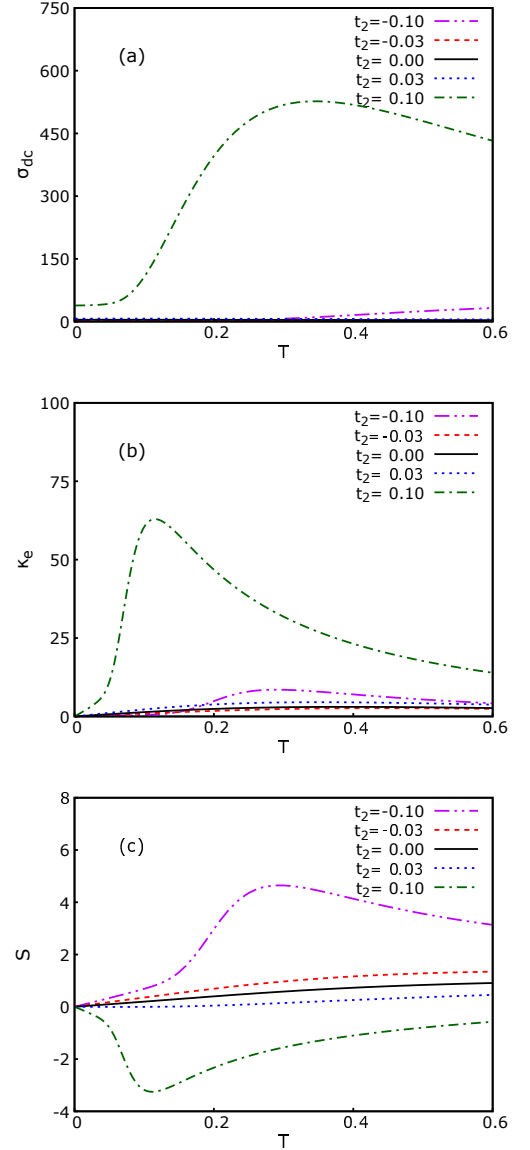


FIG. 6. (Color online) Temperature dependences of the dc conductivity σ_{dc} , thermal conductivity κ_e , and the Seebeck coefficient S is shown for the same parameters as in Fig. 5.

level reduces the dc conductivity and the thermal conductivity at low temperatures, whereas it increases the thermopower due to the asymmetry of $I(\omega)$ around the chemical potential (see Fig. 8). At high temperatures, when the gap is small with respect to $k_B T$, the doped metallic or semiconductor behavior is restored.

At half-filling and $t^{++} \neq 0$, the gap closes rapidly and the DOS exhibits a smooth peak around the chemical potential. For negative t^{++} ($t_2 < -0.5$), the gap is closed and the transport function is smooth, which results in the metallic behavior. For positive t^{++} ($t_2 > -0.5$), the transport function acquires a resonant peak which enhances the transport coefficients at low temperatures (see Fig. 8).

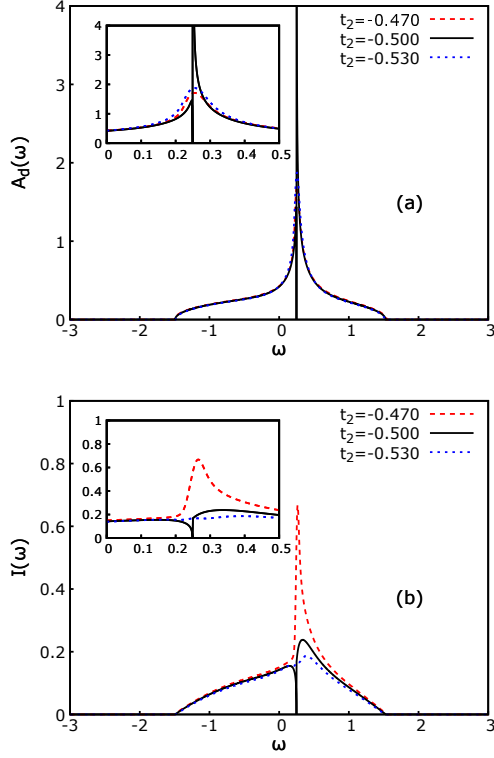


FIG. 7. (Color online) The interacting DOS (panel a) and the transport function (panel b) plotted versus ω for $U = 0.25$ at half filling ($n_f = n_d = 1/2$) and for $t_2 = -0.47, -0.5, -0.53$ ($t_3 = 0$).

Away from half filling, the three band structure of $A_d(\omega)$ emerges for small values of t^{++} (see Fig. 1). At $t^{++} = 0$ ($t_2 = -0.5$) exactly (see Fig. 9), $A_d(\omega)$ exhibits two broad bands [the lower (1) and the upper (2) Hubbard bands with spectral weights $1 - n_f$], and a δ -peak (3) at $\omega = U$ which is due to the band of localized d -states with a spectral weight $2n_f - 1$. Because we are considering the case $n_d = 1 - n_f$, the Fermi level is in the gap between the lower Hubbard band and the localized one. Unlike the single particle DOS, the transport function $I(\omega)$ has only two contributions which are due to the lower and upper Hubbard band. The absence of any feature at $\omega = U$ is obvious, if we recall that for $2n_f - 1 > 0$, the third band in $A_d(\omega)$ is due to the localized d -states in the clusters of lattice sites occupied by f -electrons. Since these localized states do not contribute much to the charge or heat transport, the shape of $I(\omega)$ and the temperature dependences of the transport coefficients (see Fig. 10) is similar to the one obtained for a doped Mott insulator.^{35,42,43}

Away from half-filling and for $t^{++} \neq 0$ (Fig. 9), the δ -peak of localized d -states (3) first broadens in a band which merges with the upper Hubbard band for larger values of $|t^{++}|$. The contribution of the localized state to transport function depends on the sign of t^{++} . For negative values of $t^{++} < 0$ ($t_2 < -0.5$), the contribution

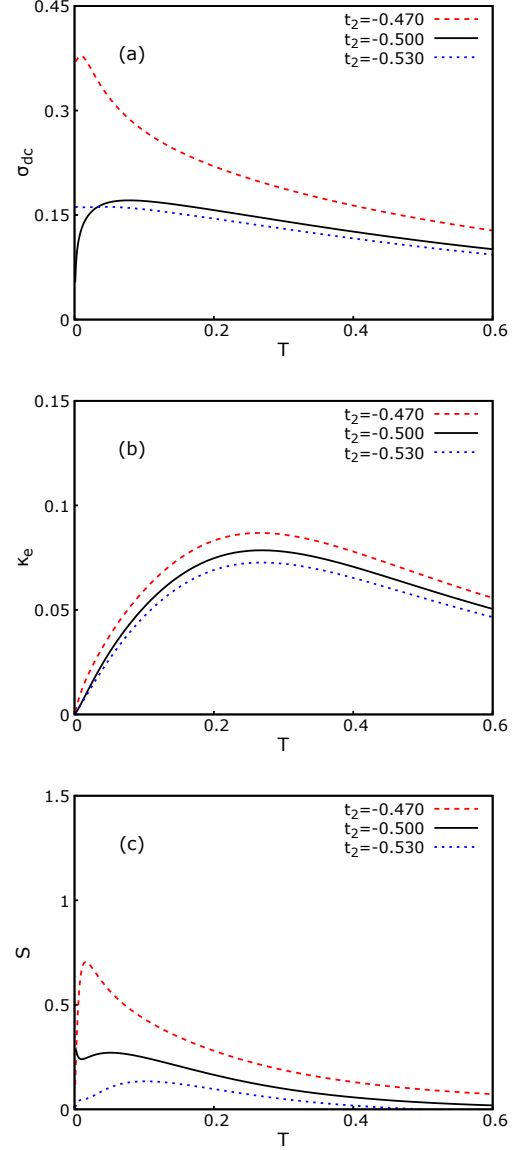


FIG. 8. (Color online) Temperature dependences of the (a) dc conductivity σ_{dc} , (b) thermal conductivity κ_e , and (c) Seebeck coefficient S is shown for the same parameters as in Fig. 7.

of localized band to the transport function first increases and then, after the localized band merges with the upper one, decreases. For $t^{++} > 0$ ($t_2 > -0.5$), the resonant peak due to the localized states dominates the transport function. In both cases, the thermoelectric properties are enhanced; most prominently for positive t^{++} , when the resonant peak affects strongly the transport properties (see Fig. 10).

2. Strongly correlated hopping

A large enough increase of the local Coulomb interaction U leads to the reconstruction of the DOS and trans-

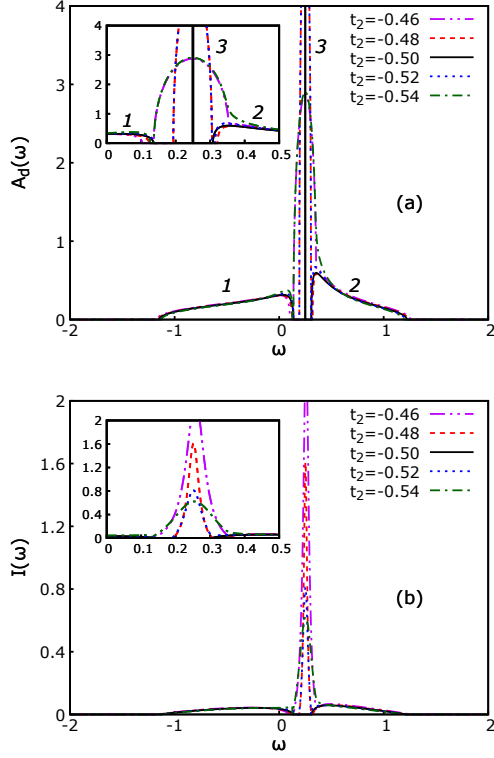


FIG. 9. (Color online) The interacting DOS (panel a) and the transport function (panel b) plotted versus ω for $U = 0.25$, $n_f = 0.75$, $n_d = 1 - n_f = 0.25$, and for $t_2 = -0.46, -0.48, -0.50, -0.52, -0.54$. Labels 1, 2, and 3 denote the lower Hubbard band, the upper Hubbard band, and band of localized states, respectively.

port function. The Mott-Hubbard gap becomes large and governs the transport properties at low temperatures. Besides, the upper Hubbard band becomes narrow with a high density of states. At half filling and $t^{++} = 0$ ($t_2 = -0.5$), the upper Hubbard band has a singularity at the bottom edge, whereas the transport function shows only a step-like feature at this frequency (Fig. 11). The temperature dependences of dc charge and thermal conductivities are similar to the one for doped Mott insulators,^{35,42,43} but the Seebeck coefficient behaves differently: it is negative and displays anomalous behavior at low temperatures reflecting an anomalous temperature dependence of chemical potential forced by the singularity on DOS (Fig. 12). For the nonzero values of t^{++} , the features in the upper Hubbard band are blurred, both for the DOS and for the transport function. Again, for the positive values of $t^{++} > 0$ ($t_2 > -0.5$), the resonant peak gives a dominant contribution to the transport function, which leads to an increase of dc charge and thermal conductivities and makes Seebeck coefficient positive, shifting its anomalous behavior to lower temperatures.

An increase of doping leads, in the narrow interval of t^{++} values around $t^{++} = 0$ ($t_2 = -0.5$), to the three-band structure in the DOS and the transport function

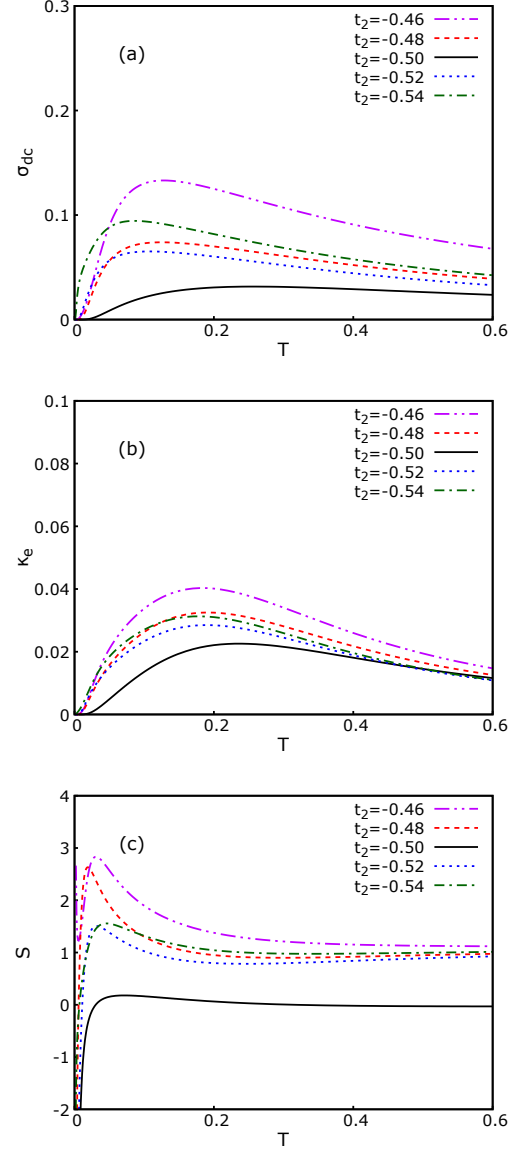


FIG. 10. (Color online) Temperature dependence of the (a) dc conductivity σ_{dc} , (b) thermal conductivity κ_e , and (c) Seebeck coefficient S in the weak coupling regime is shown for the same parameters as in Fig. 9.

[the lower Hubbard band, the upper Hubbard band, and the band of localized states are shown in Fig. 13(a) by the lines (1), (2), and (3), respectively]. At $t^{++} = 0$, the DOS acquires a δ -peak [shown by vertical line (3) in Fig. 13(a)] coming from the localized d -states which do not contribute to transport. Any deviation of t^{++} from zero broadens the δ -peak in a narrow band which affects the transport (see Fig. 14). At sufficiently large value of $|t^{++}|$ the band of localized states [line (3) in Fig. 13] merges with the upper Hubbard band [line (2)], so that the sharp features in DOS are blurred. Here, the resonant peak gives the main contribution to transport function, which is large for positive t^{++} ($t_2 > -0.5$) and

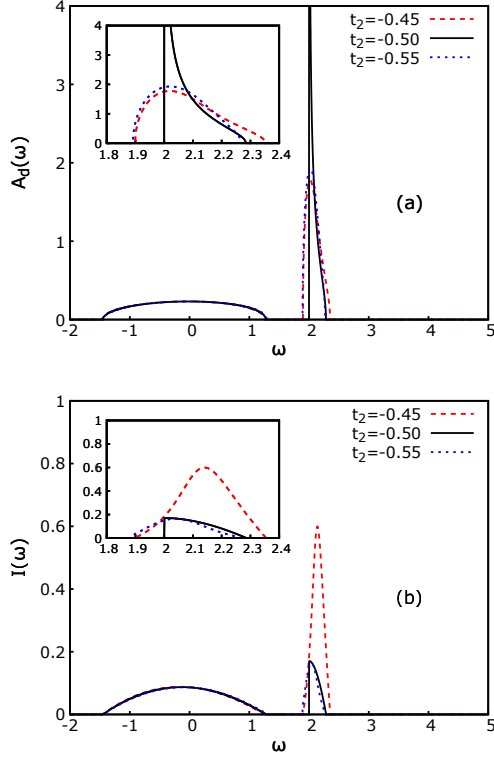


FIG. 11. (Color online) The interacting DOS (panel a) and the transport function (panel b) is plotted versus ω for $U = 2$ at half filling ($n_f = n_d = 1/2$) and for $t_2 = -0.45, -0.5, -0.55$ ($t_3 = 0$).

much smaller for negative one ($t_2 < -0.5$). This leads to an increase of the dc charge and thermal conductivity, and to the change of the temperature dependence of the Seebeck coefficient, which is now large and positive.

V. DISCUSSION AND CONCLUSIONS

In this article we studied the effects of correlated hopping on the density of states and transport coefficients of a strongly correlated material described by the Falicov-Kimball model. An exact solution for the one particle and two particle quantities are obtained within the dynamical mean field theory for the Bethe lattice with a semielliptic density of states.

First, we have analyzed an influence of correlated hopping on the behavior of the renormalized DOS $A_d(\omega)$ and transport function $I(\omega)$ which defines the transport coefficients via the Boltzmann relations (Jonson-Mahan theorem). Both quantities have the same band edges but completely different shapes. The renormalized DOS reflects the single particle properties and the main effect of correlations is an effective narrowing of the band widths with the simultaneous creation of the Mott gap and the appearance of the band of localized states with doping. On the other hand, the transport function $I(\omega)$ reflects

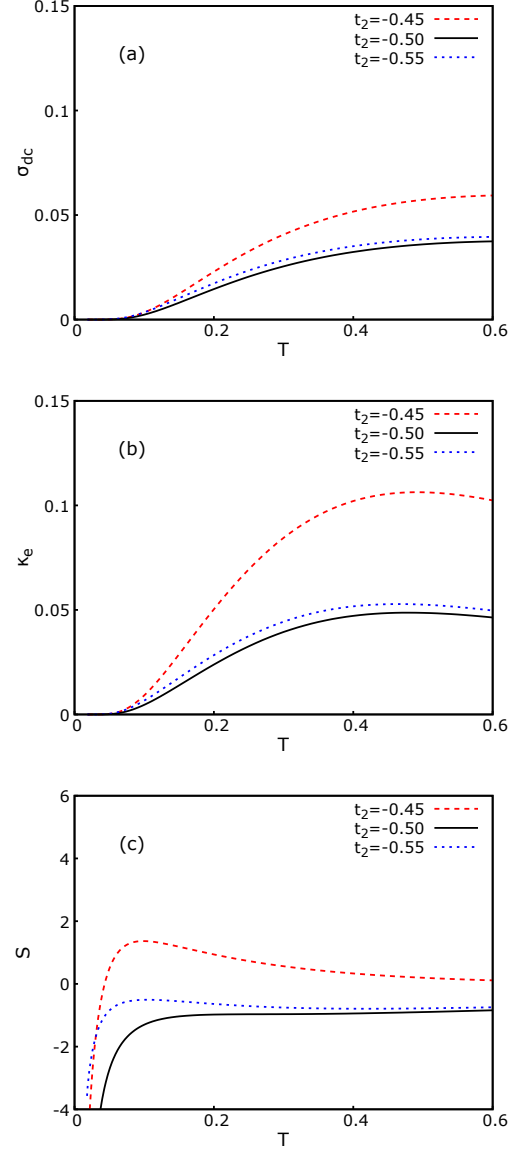


FIG. 12. (Color online) Temperature dependence of the dc conductivity σ_{dc} , the thermal conductivity κ_e , and Seebeck coefficient S in the strong coupling regime is shown for the same parameters as in Fig. 11.

the two-particle correlations and its behavior is dominated by the resonant contribution. The fact that the resonant peak continuously enters the region of the one-particle localization for small values of $|t^{++}|$ allows us to conjecture that it derives from the two particle interference in random media, e.g., weak (anti)localization.⁴⁴ In certain sense, the correlated hopping mimics the random media, with different values of the hopping integral corresponding to the random distances between the atoms. From this point of view, the condition of resonance (44) corresponds to the interference condition for the single particle excitations following different trajectories over the sites which are either occupied or unoccupied by the

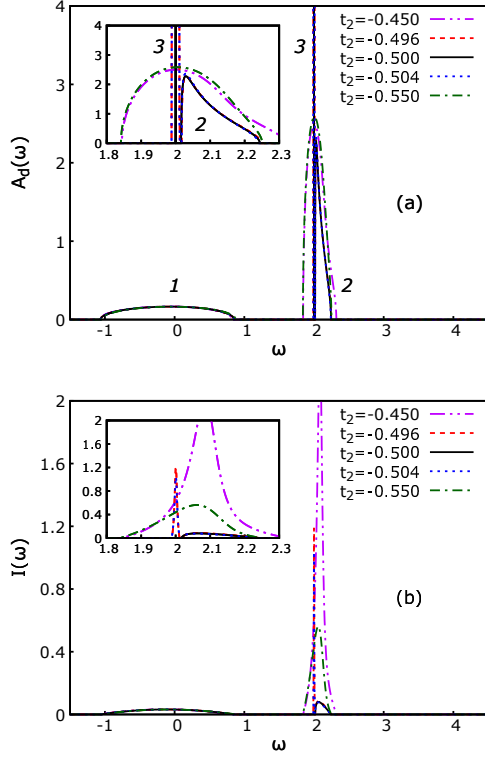


FIG. 13. (Color online) The interacting DOS (panel a) and the transport function (panel b) for $U = 2$ and $n_f = 0.75$, and $n_d = 1 - n_f = 0.25$. Here, $t_2 = -0.45, -0.496, -0.5, -0.504, -0.55$ and labels 1, 2, and 3 denote the lower Hubbard band, the upper Hubbard band, and the band of localized states, respectively.

f -particles.

In our previous article,³³ we found that the charge and heat transport of the particles described by the Falicov-Kimball model on a hypercubic lattice exhibit a number of surprising features and assumed that these anomalies are mainly due to the peculiarities of the Gaussian density of states, which does not have the clear-cut band edges and never vanishes. To our surprise, similar behavior is obtained for the Bethe lattice with the semi-elliptic density of states, so that the anomalous behavior of transport coefficients seems to be a common feature of systems with correlated hopping.

For a wide range of the hopping parameter, t_2 , we find that the anomalous features of $I(\omega)$ are due to the resonant two particle contribution. Contrary to that, the renormalized one particle DOS does not display any anomalies. The analytic expression for the resonant frequency, Eq. (45), shows that by tuning the concentration of the itinerant electrons we can bring the Fermi level in the proximity of the resonance and increase substantially the conductivities and the thermoelectric power. We also show that the reduction of the amplitude of correlated hopping between the sites occupied by the f particles, $t^{++} \rightarrow 0$, creates a band of d states localized in the clus-

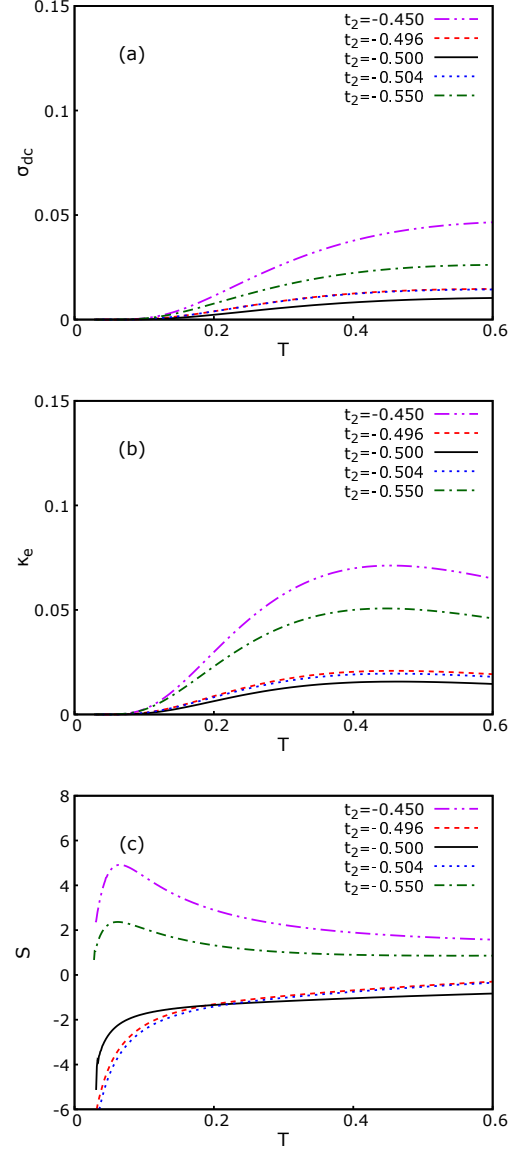


FIG. 14. (Color online) Temperature dependence of the dc conductivity σ_{dc} , the thermal conductivity κ_e , and Seebeck coefficient S for the same parameters as in Fig. 13.

ters of sites occupied by the f electrons. For the f electron concentrations above the half filling, $n_f > 0.5$, this band contributes to the single particle DOS, in addition to the lower and upper Hubbard bands. Depending on the d electron concentration, the Fermi level for itinerant electrons can overlap either the lower ($n_d < 1 - n_f$) or the upper ($n_d > n_f$) Hubbard band or the band of localized states ($1 - n_f < n_d < n_f$). In each of these cases, the thermoelectric coefficients exhibit a completely different behavior.

Finally, we remark that a strong enhancement of the conductivities by correlated hopping, driven by the two-particle resonant states, has been found for the Falicov-Kimball model with static interaction. It would be of

great interest to check whether similar transport anomalies emerge in the models with dynamic interactions, e.g. in the Hubbard model with correlated hopping, including the one with the Fermi liquid or the superconducting ground state.^{5,6}

ACKNOWLEDGMENTS

V.Z. acknowledges the support by the Ministry of Science of Croatia under the bilateral agreement with the USA on the scientific and technological cooperation, Project No. 1/2014.

- ¹ J. Hubbard, “Electron correlations in narrow energy bands,” *Proc. R. Soc. Lond. A* **276**, 238–257 (1963).
- ² M. E. Foglio and L. M. Falicov, “New approach to the theory of intermediate valence. I. General formulation,” *Phys. Rev. B* **20**, 4554–4559 (1979).
- ³ M. E. Simón and A. A. Aligia, “Brinkman-Rice transition in layered perovskites,” *Phys. Rev. B* **48**, 7471–7477 (1993).
- ⁴ The name used for such contributions is not well established yet. Apart from the term “correlated hopping”, many other terms circulate, such as “assisted hopping”, “bond-charge interaction (repulsion)”, “occupation-dependent hopping”, “correlated hybridization”, etc. Similar contributions in the theory of disordered systems are also known as an “off-diagonal disorder”³¹.
- ⁵ J. E. Hirsch, “Bond-charge repulsion and hole superconductivity,” *Physica C* **158**, 326–336 (1989).
- ⁶ Bogdan R. Bulka, “Superconductivity in the Hubbard model with correlated hopping: Slave-boson study,” *Phys. Rev. B* **57**, 10303–10306 (1998).
- ⁷ Liliana Arrachea, E. R. Gagliano, and A. A. Aligia, “Ground-state phase diagram of an extended Hubbard chain with correlated hopping at half-filling,” *Phys. Rev. B* **55**, 1173–1184 (1997).
- ⁸ Masahisa Tsuchiizu, Yukiko Omori, Yoshikazu Suzumura, Marie-Laure Bonnet, and Vincent Robert, “Ab initio derivation of multi-orbital extended Hubbard model for molecular crystals,” *The Journal of Chemical Physics* **136**, 044519 (2012), 10.1063/1.3678307.
- ⁹ L. Didukh, Yu. Skorenkyy, Yu. Dovhopyaty, and V. Hankevych, “Metal-insulator transition in a doubly orbitally degenerate model with correlated hopping,” *Phys. Rev. B* **61**, 7893–7908 (2000).
- ¹⁰ M. Kollar and D. Vollhardt, “Correlated hopping of electrons: Effect on the Brinkman-Rice transition and the stability of metallic ferromagnetism,” *Phys. Rev. B* **63**, 045107 (2001).
- ¹¹ Yigal Meir, Kenji Hirose, and Ned S. Wingreen, “Kondo model for the “0.7 anomaly” in transport through a quantum point contact,” *Phys. Rev. Lett.* **89**, 196802 (2002).
- ¹² A. Hübsch, J. C. Lin, J. Pan, and D. L. Cox, “Correlated hybridization in transition-metal complexes,” *Phys. Rev. Lett.* **96**, 196401 (2006).
- ¹³ S. B. Tooski, A. Ramšak, B. R. Bulka, and R. Žitko, “Effect of assisted hopping on thermopower in an interacting quantum dot,” *New J. Phys.* **16**, 055001 (2014).
- ¹⁴ Ole Jürgensen, Klaus Sengstock, and Dirk-Sören Lühmann, “Density-induced processes in quantum gas mixtures in optical lattices,” *Phys. Rev. A* **86**, 043623 (2012).
- ¹⁵ M. Di Liberto, C. E. Creffield, G. I. Japaridze, and C. Morais Smith, “Quantum simulation of correlated-hopping models with fermions in optical lattices,” *Phys. Rev. A* **89**, 013624 (2014).
- ¹⁶ María Eckholt and Juan José García-Ripoll, “Correlated hopping of bosonic atoms induced by optical lattices,” *New J. Phys.* **11**, 093028 (2009).
- ¹⁷ Dirk-Sören Lühmann, Ole Jürgensen, and Klaus Sengstock, “Multi-orbital and density-induced tunneling of bosons in optical lattices,” *New Journal of Physics* **14**, 033021 (2012).
- ¹⁸ Ole Jürgensen, Florian Meinert, Manfred J. Mark, Hanns-Christoph Nägerl, and Dirk-Sören Lühmann, “Observation of density-induced tunneling,” *Phys. Rev. Lett.* **113**, 193003 (2014).
- ¹⁹ L. M. Falicov and J. C. Kimball, “Simple model for semiconductor-metal transitions: SmB_6 and transition-metal oxides,” *Phys. Rev. Lett.* **22**, 997–999 (1969).
- ²⁰ Z. Gajek and R. Lemański, “Correlated hopping in the 1D Falicov-Kimball model,” *Acta Phys. Pol. B* **32**, 3473–3476 (2001).
- ²¹ J. Wojtkiewicz and R. Lemański, “Ground states of the Falicov-Kimball model with correlated hopping,” *Phys. Rev. B* **64**, 233103 (2001).
- ²² J. Wojtkiewicz and R. Lemański, “2D Falicov-Kimball model with correlated hopping in the large U limit,” *Acta Phys. Pol. B* **32**, 3467–3472 (2001).
- ²³ H. Čenčariková and P. Farkašovsky, “Formation of charge and spin ordering in strongly correlated electron systems,” *Condens. Matter Phys.* **14**, 42701 (2011).
- ²⁴ Walter Metzner and Dieter Vollhardt, “Correlated hopping of lattice fermions in $d = \infty$ dimensions,” *Phys. Rev. Lett.* **62**, 324–327 (1989).
- ²⁵ U. Brandt and C. Mielsch, “Thermodynamics and correlation functions of the Falicov-Kimball model in large dimensions,” *Zeitschrift für Physik B Condensed Matter* **75**, 365–370 (1989).
- ²⁶ Antoine Georges, Gabriel Kotliar, Werner Krauth, and Marcelo J. Rozenberg, “Dynamical mean-field theory of strongly correlated fermion systems and the limit of infinite dimensions,” *Rev. Mod. Phys.* **68**, 13–125 (1996).
- ²⁷ J. K. Freericks and V. Zlatić, “Exact dynamical mean-field theory of the Falicov-Kimball model,” *Rev. Mod. Phys.* **75**, 1333–1382 (2003).
- ²⁸ Avraham Schiller, “Correlated hopping in the Falicov-Kimball model: A large-dimensions study,” *Phys. Rev. B* **60**, 15660–15663 (1999).
- ²⁹ Andrij M. Shvaika, “Dynamical mean-field theory of correlated hopping: A rigorous local approach,” *Phys. Rev. B* **67**, 075101 (2003).
- ³⁰ Andrij M. Shvaika, “Erratum: Dynamical mean-field theory of correlated hopping: A rigorous local approach [Phys. Rev. B **67**, 075101 (2003)],” *Phys. Rev. B* **82**, 119901 (2010).
- ³¹ J. A. Blackman, D. M. Esterling, and N. F. Berk, “Generalized locator—coherent-potential approach to binary al-

- loys,” *Phys. Rev. B* **4**, 2412–2428 (1971).
- ³² Kozo Hoshino and Komajiro Niizeki, “The CPA calculation of the thermoelectric power of a binary alloy with off-diagonal disorder,” *J. Phys. Soc. Jpn.* **38**, 1320–1327 (1975).
- ³³ A. M. Shvaika, “Effect of correlated hopping on thermoelectric properties: Exact solutions for the Falicov-Kimball model,” *Condens. Matter Phys.* **17**, 43704 (2014).
- ³⁴ J. K. Freericks, D. O. Demchenko, A. V. Joura, and V. Zlatić, “Optimizing thermal transport in the Falicov-Kimball model: The binary-alloy picture,” *Phys. Rev. B* **68**, 195120 (2003).
- ³⁵ A. V. Joura, D. O. Demchenko, and J. K. Freericks, “Thermal transport in the Falicov-Kimball model on a Bethe lattice,” *Phys. Rev. B* **69**, 165105 (2004).
- ³⁶ Walter Metzner, “Linked-cluster expansion around the atomic limit of the Hubbard model,” *Phys. Rev. B* **43**, 8549–8563 (1991).
- ³⁷ M. Jonson and G. D. Mahan, “Mott’s formula for the thermopower and the Wiedemann-Franz law,” *Phys. Rev. B* **21**, 4223–4229 (1980).
- ³⁸ M. Jonson and G. D. Mahan, “Electron-phonon contribution to the thermopower of metals,” *Phys. Rev. B* **42**, 9350–9356 (1990).
- ³⁹ J. K. Freericks, V. Zlatić, and A. M. Shvaika, “Electronic thermal transport in strongly correlated multilayered nanostructures,” *Phys. Rev. B* **75**, 035133 (2007).
- ⁴⁰ Louis-François Arsenault and A.-M. S. Tremblay, “Transport functions for hypercubic and Bethe lattices,” *Phys. Rev. B* **88**, 205109 (2013).
- ⁴¹ Woonki Chung and J. K. Freericks, “Charge-transfer metal-insulator transitions in the spin- $\frac{1}{2}$ Falicov-Kimball model,” *Phys. Rev. B* **57**, 11955–11961 (1998).
- ⁴² V. Zlatić and J. K. Freericks, “Strongly enhanced thermal transport in a lightly doped Mott insulator at low temperature,” *Phys. Rev. Lett.* **109**, 266601 (2012).
- ⁴³ V. Zlatić, G. R. Boyd, and J. K. Freericks, “Universal thermopower of bad metals,” *Phys. Rev. B* **89**, 155101 (2014).
- ⁴⁴ Gerd Bergmann, “Physical interpretation of weak localization: A time-of-flight experiment with conduction electrons,” *Phys. Rev. B* **28**, 2914–2920 (1983).